HAL
open science

Validation of TRF-E as gasoline surrogate through an experimental laminar burning speed investigation

Marco Di Lorenzo, Pierre Brequigny, Fabrice Foucher, Christine Mounaïm-Rousselle

To cite this version:

Marco Di Lorenzo, Pierre Brequigny, Fabrice Foucher, Christine Mounaïm-Rousselle. Validation of TRF-E as gasoline surrogate through an experimental laminar burning speed investigation. Fuel, 2019, 253, pp.1578-1588. 10.1016/j.fuel.2019.05.081 . hal-02150886

HAL Id: hal-02150886

https://hal.science/hal-02150886v1

Submitted on 7 Jun 2019

HAL is a multi-disciplinary open access archive for the deposit and dissemination of scientific research documents, whether they are published or not. The documents may come from teaching and research institutions in France or abroad, or from public or private research centers.

L'archive ouverte pluridisciplinaire **HAL**, est destinée au dépôt et à la diffusion de documents scientifiques de niveau recherche, publiés ou non, émanant des établissements d'enseignement et de recherche français ou étrangers, des laboratoires publics ou privés.

Validation of TRF-E as gasoline surrogate through an experimental laminar burning speed investigation

M.Di Lorenzo, P.Brequigny, F.Foucher, C.Mounaïm-Rousselle

Université d'Orléans, INSA-CVL, PRISME, EA 4229, F45072 Orléans, France

1. Introduction

In the road transport sector, it is more and more evident that spark ignition (SI) engines fuelled with gasoline will remain the main powertrain for the next decades, even incorporated in hybrid electric vehicles. This is why one main challenge concerns the increase of efficiency to improve the fuel economy and decrease pollutant emissions. Due to the highly advanced technology reached in the current state of art of ICEs, it appears clear that the major route towards a high efficiency SI engine is downsizing, which consists in increasing the engine load through displacement reduction and turbocharging. As this leads to an increase of initial temperature and pressure, high level of dilution has to be used to avoid abnormal combustions. But, as the stability of the premixed turbulent combustion is strongly affected by dilution, increasing the tolerance of SI engines to high dilution percentages remains a major technical challenge. The prediction of engine behavior in these working mode conditions remains not sufficiently accurate. Most of turbulent premixed combustion models are based on the flamelets regime assumption [1]. However, recent work of Mounaïm-Rousselle et al. [2] pointed out a possible breach of this regime in Spark-Ignition (SI) engines for particular operating conditions, such as downsized engines with high rates of exhaust gas recirculation (EGR) [3], [4]. According to the flamelets model, the flame is considered as asymptotically thin and locally laminar even if the turbulence can wrinkle the flame surface [5], [6]. That explains why laminar burning velocity is a crucial factor in most practical combustion systems and its investigation is still an open research field. Moreover, even though this parameter depends on equivalence ratio, pressure, temperature and diluent gases in the mixture [7], [8], its value is basically a strict characteristic of the fuel itself. To evaluate potential alternative fuels and/or suitable surrogate [9]–[11], the acquisition of complete laminar burning velocities database is required before having access to accurate kinetics mechanism.

Commercial gasoline is composed by hundreds of different chemical species that severely increase the complexity, including experimental or numerical approaches [12]. Using surrogate fuel, with well-known

composition, allows reducing the complexity to identify the key mechanisms of the reactive mixture [12], [13]. Nonetheless, the surrogate must be representative of the target gasoline. It can be single or multi-components, depending on the purpose of the investigation. As single-component surrogate, iso-octane is widely used for gasoline fuel and may be representative for fundamental phenomena analysis[14]. Nevertheless, Stanglmainer et al. [15] pointed out that the differences between gasoline and iso-octane can be significant at high pressure and temperature. Thus, when the surrogates have to explicitly represent the gasoline behavior, the association through the research octane number (RON) is a practical solution. This coupling is obtained by mixing iso-octane and n-heptane, leading to the Primary Reference Fuels (PRFs) that represent suitable surrogates for gasolines under certain conditions [12], [14], [16]. For example, Jerzembeck et al. [17] compared a commercial gasoline with a PRF mixture characterized by RON 87, deducing that the agreement between the two fuels decreases with increasing equivalence ratio. Similarly, Bradley et al. investigated laminar burning velocities of different PRFs up to 1.0 MPa [18], [19]. However, Cruz et al. [13] and Farrell et al. [20] highlighted the fact that PRFs can considerably differ from a pure gasoline due to the different combustion properties of aromatic species with respect to alkanes. Therefore, in order to simulate refinery gasoline, surrogates that include a certain percentage of toluene in the composition represent the actual reference [12]. These are called Toluene Reference Fuels (TRFs) and the best composition in order to fit the gasoline properties is still an open topic as strictly depending on the gasoline target. However, multi-components surrogates of three or more species are the best option when the target is to develop, for example, advanced chemical kinetics mechanisms. Even if several studies have investigated the flame characteristics of different hydrocarbons used in multi-components surrogates [21]–[23], less studies focused on the determination of the laminar burning velocity for gasoline and TRFs, pure [11], [21] or eventually blended with other species (*e.g.* ethanol) [24], [25], are available on the literature. The aim of the present work is first to validate a specially designed surrogate, the TRF-E (i.e. a blend of TRF with ethanol), as a surrogate of the commercial gasoline (*B71 1188 ESSH EURO5 +20, RON 96.6 MON 86.2, Ethanol 5%vol).* And, secondly, to provide TRF-E

GASOLINE		TRF-E	
RON	96.6	**RON**	95
%C, %H, % O (%mass)	85.1/13.1/1.8	**%C, %H, % O (%mass)**	84.79/13.34/1.87
$\boldsymbol{\rho}$ $(\boldsymbol{kg/m^3})$	753.0	$\boldsymbol{\rho}$ $(\boldsymbol{kg/m^3})$	750.5
Ethanol (%vol)	5.0	Ethanol (%vol)	5.0
n-Heptane (%vol)	3.6	*n*-Heptane (%vol)	15.0
Olefin (%vol)	6.2	*iso*-Octane (%vol)	44.0
Aromatic (%vol)	33.7	Toluene (%vol)	36.0
Benzene (%vol)	0.1	-	
Methyl-cyclohexane (%vol)	1.5	-	

Table 1: Properties and composition of the gasoline (B71 1188 ESSH EURO5 +20) and its surrogate TRF-E.

laminar burning velocity database to allow the development of the accurate kinetics mechanism. Effects of pressure, aromatic compounds oxidation and high EGR percentages, in particular, are critical in the development of kinetics mechanisms [26]. It is then fundamental to provide experimental data concerning the combination of all these factors. In fact, current literature includes several studies on mono-component fuels or PRF surrogates diluted by CO_2, N_2, H_2O or a combination of those, like synthetic EGR [7], [8], [27]–[31]. In this sense remarkable work was conducted by Marshall et al. [32] using real combustion residuals as diluent with several mono-component fuels. Nonetheless, there is still a lack of data regarding more complex fuels diluted by EGR. Recently, Mannaa et al. [33] provided a deep investigation on the influence of ethanol and dilution on a gasoline and its surrogate, using real EGR. It was figured out that significant percentages of ethanol (up to 85%) may mitigate the flame speed reduction caused by EGR dilution. Moreover, a stabilization effect due to EGR was observed, comparing delays in the cellularity arising and Markstein lengths of the different blends. As reported in Table 1, the present work focused on a surrogate with relatively low ethanol percentage (5%) and significant toluene percentage (36%). Then, the TRF-E validation and characterization will be crucial in the development of accurate kinetics mechanism, allowing the investigation of aromatics oxidation, high multi-species diluent rate and high pressure effects on the chemistry. On the other hand, the present work aims to furnish the literature with a refined mathematical correlation for laminar burning velocity prediction of TRFE/air/EGR and gasoline/air/EGR blends.

2. Experimental Setup

Reference conditions were fixed at 473 K, 0% EGR dilution and 0.1 MPa. The two fuels were compared for each combination of dilution and pressure at 473 K. Then, the effect of the temperature was evaluated by adding

other two experimental points (373 and 423 K) at 0.1 MPa and 0% EGR. The equivalence ratio (ϕ) was varied between 0.8 and 1.3. Three tests were performed for each condition. Once the surrogate validation was accomplished through this first investigation, the TRF-E database was widened with the addition of two other values of temperature, 373 and 423 K for the same combination of pressure, dilution and equivalence ratio. This wide range of experimental points allows to deeply evaluate the mathematical correlation initially proposed by [34] and widely used in previous works [7], [8]. Details on the investigated experimental conditions are reported in Table 2.

The experimental setup used in the present work allows both laminar and turbulent flame propagation investigation as described in Galmiche et al. [7]. The combustion chamber is a spherical stainless steel vessel with an inner volume of 4.2 l, and an inner diameter of 200 mm. The vessel is equipped with four quartz windows of 70

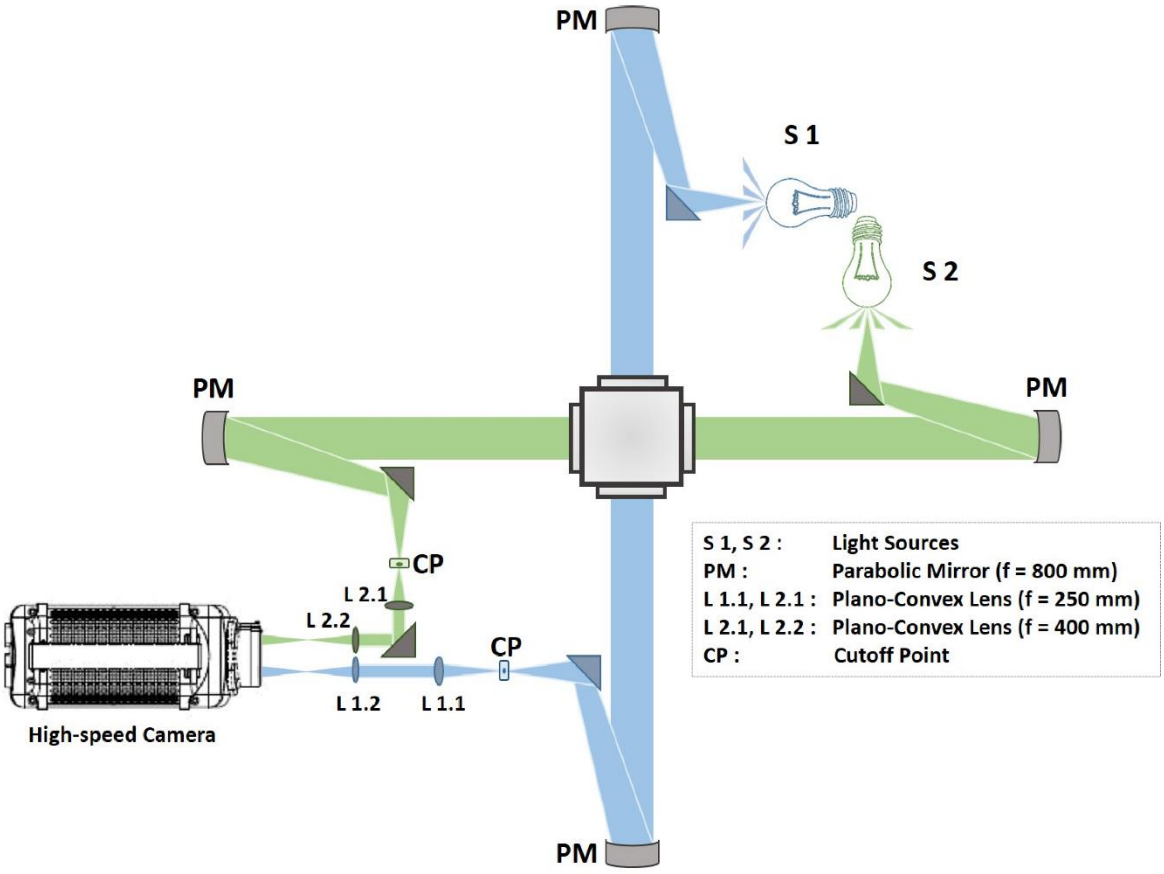

Figure 1: Scheme of the Double-View Schlieren configuration using one high-speed camera for two transversal profiles of the flame.

Dilution	Pressure / Temp.	1 bar	2 bar	3 bar	5 bar
0% EGR	***373 K***	TRF-E & Gasoline	TRF-E	TRF-E	TRF-E
	423 K	TRF-E & Gasoline	TRF-E	TRF-E	TRF-E
	473 K	TRF-E & Gasoline	TRF-E & Gasoline	TRF-E & Gasoline	TRF-E & Gasoline
10% EGR	***373 K***	TRF-E	TRF-E	TRF-E	TRF-E
	423 K	TRF-E	TRF-E	TRF-E	TRF-E
	473 K	TRF-E & Gasoline	TRF-E & Gasoline	TRF-E & Gasoline	TRF-E & Gasoline
20% EGR	***373 K***	TRF-E	TRF-E	TRF-E	TRF-E
	423 K	TRF-E	TRF-E	TRF-E	TRF-E
	473 K	TRF-E & Gasoline	TRF-E & Gasoline	TRF-E & Gasoline	TRF-E & Gasoline

Table 2: Investigated experimental conditions, for each combination of pressure, temperature and EGR dilution, three test were performed at different Equivalence Ratio (0.8, 0.9, 1.0, 1.1, 1.2, and 1.3).

mm diameter. A heater wire resistance is placed on the outer surface to heat the chamber up to 473 K. A vacuum pump is used to extract all the gases before starting each test, until reach a minimal pressure of 0.005 bar. After that, a set of gaseous flowmeters (Brooks 5850S, 2 NL/min for air, 0.5 NL/min for CO_2 and 0.5 NL/min for N_2) allows to inject the different gases according to the desired composition. In this respect, the composition of the synthetic air is 20.9% O2 and 79.1% N2. In parallel, two liquid flowmeters (Bronkhorst mini CORI-FLOW 30 g/h) inject the fuel and the water that is requested in the diluent composition. According to the composition of the burned gases in a stoichiometric flame air/TRF-E, the EGR composition is 13.62% CO_2, 12.22% H_2O and 74.16% N_2. The liquid intakes are heated in order to grant a minimal vaporization temperature of 373 K. Inside the combustion chamber a fan assures the homogeneity of the gaseous mixture consequently to the injection. Anyway, the fan is stopped 10 s before the ignition in order to grant that the flow is at rest, avoiding the development of turbulent perturbations. The ignition is realized through two tungsten electrodes, with a diameter of 0.5 mm and distant 1.5 mm each other, powered by a conventional capacitive discharge ignition system. The charging time of the ignition coil is set to 3 ms in the present experiments, resulting in a discharge energy of about 100 mJ. Further details on the ignition system can be found in [7], [8], [27]. For each test, a maximum tolerance of 3% was accepted for the initial pressure, while for the temperature 2 K with respect to the fixed value. The flowmeters accuracy settles at

±0.5% of the maximum range. This usually produces a slight excess in the actual injected quantities with respect to the set point. After each test, quantities of liquids and gases injected are verified, to determine the real equivalence ratio at which the experiment was performed. The maximum error can be considered as 5% with respect to the nominal value. For all data provided in the following, real values of equivalence ratio are considered and not the nominal ones.

3. Optical Technique and Post-process

A Double-Views Schlieren configuration was implemented in the combustion vessel to have simultaneously two different views of the flame propagation recorded in just one High Speed Phantom v1610 camera, as reported schematically in Figure 1. The aim is to evaluate the electrodes effect on the flame or the detection of possible irregularities and/or anisotropies in the flame spherical shape, by giving a tridimensional idea of the flame evolution.

Two lamps are used as light sources and a set of mirrors, both planar and convex, ensures that the light beam is, respectively, well-oriented and parallel. As reported in the scheme in Figure 1, the light is firstly directed to a parabolic mirror, with a focal length of 800 mm, that is the same distance from the light source, obtaining a parallel beam. After the combustion chamber, another parabolic mirror, equal to the first, is used to converge the light to the cutoff point. Through other two plano-convex lens (with focal length of 250 and 400 mm) the light beam path is optimized to correctly impact the camera objective with the optimal size. The frame rate was fixed at 7000 fps, with a resolution of 1280x800 pixel^2 and a ratio mm/pixel equal to 0.1097.

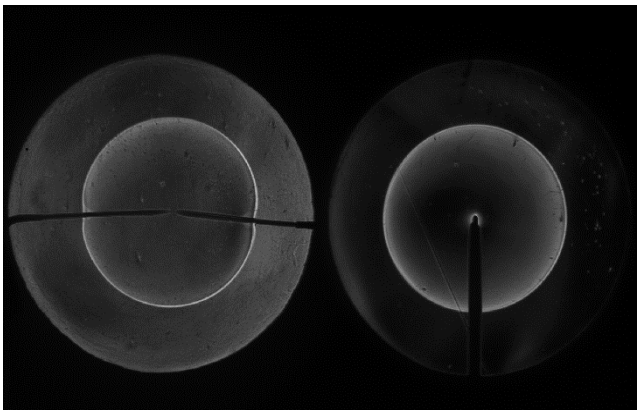

Figure 2: Example of flame visualization: TRF-E, Φ=1.1 (T = 473 K, P = 1 bar, EGR = 0%).

An example of Double-Views of flame is presented in Figure 2. The assumption of a spherical evolution of the flame is consistent. The images post-processing was performed using a MATLAB routine that subtracts the background and performs the binarization of the image. Moreover, a low pass filter is applied in order to smooth the contour and decrease the noise. From the contour, the burnt gas area is computed and, then by considering the flame spherical, an equivalent radius as

$$R_S = \sqrt{\frac{A}{\pi}} \qquad (1)$$

The maximum radius value considered for the analysis is 25 mm in order to avoid the chamber wall effect on the flame and respect the constant pressure hypothesis [7], [8], [27]. On the other hand, the minimum radius value considered is 6.5 mm due to the ignition system contribution to the initial flame propagation [35]. Within this range, the flame propagation velocity can be estimated as the time derivative of the radius

$$V_S = \frac{dr_f}{dt} \qquad (2)$$

The experimental radius R_S corresponds to the isothermal detected through the optical technique. Assuming that the flame thickness can be considered infinitesimal, this radius can be approximated with the flame front radius r_f. The stretch rate is computed as (from [36])

$$K = \frac{1}{A}\frac{dA}{dt} \qquad (3)$$

that is,

$$K = \frac{2}{r_f}\frac{dr_f}{dt} \qquad (4)$$

if a spherical expanding flame is considered [36].

Using the stretch rate and the flame speed, the unstretched laminar flame propagation velocity can be estimated through the non-linear correlation proposed by Kelley and Law [37] and methodology described by Halter al. [38].

$$\left(\frac{V_S}{V_S^0}\right)^2 ln\left(\frac{V_S}{V_S^0}\right)^2 = -\frac{2L_bK}{V_S^0} \qquad (5)$$

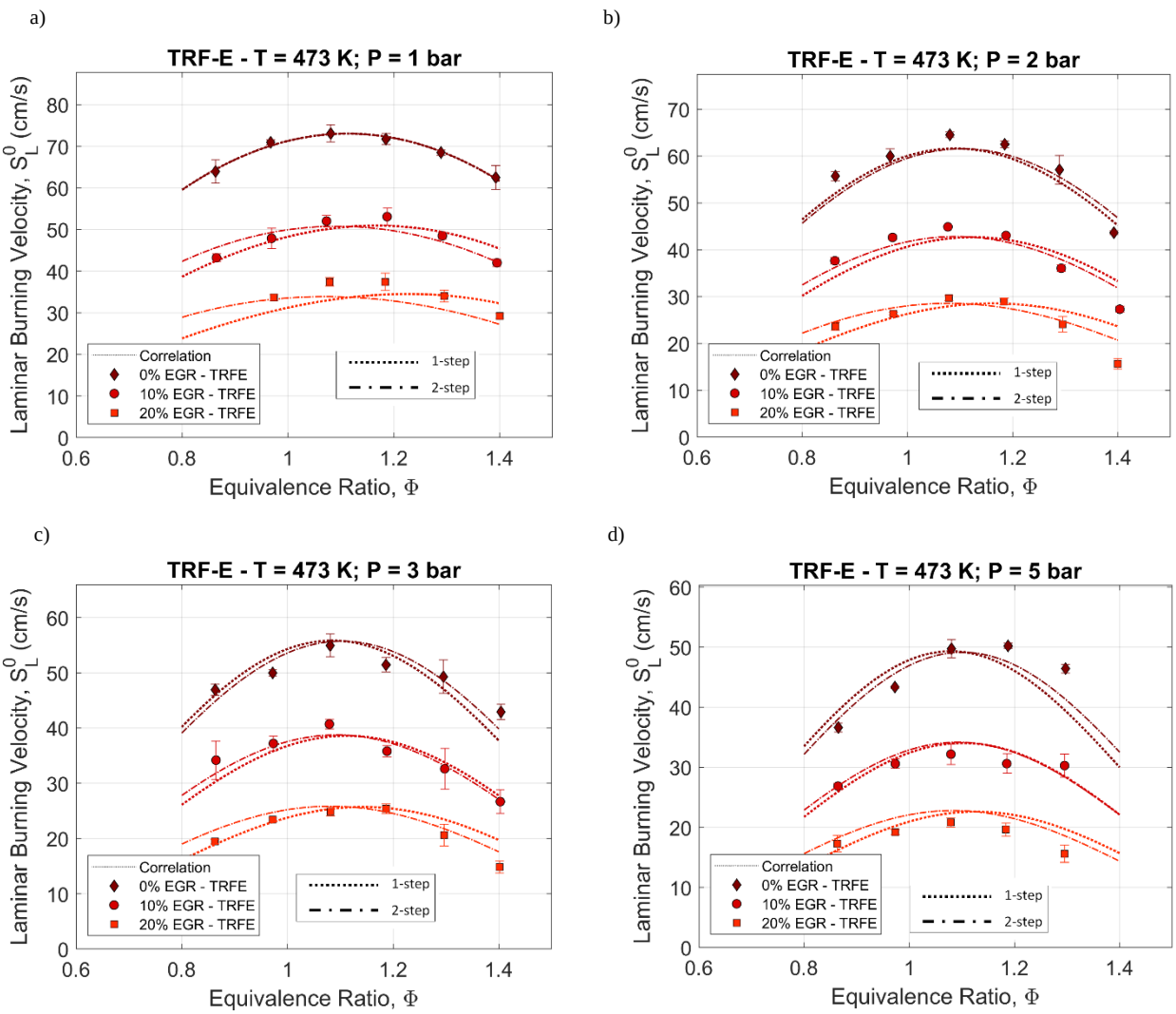

Figure 3: TRF-E laminar burning velocities at different pressure values (Figures a, b, c, d) and fixed temperature (T = 473 K) for three dilution rates: experimental points and correlation curves with comparison between 1-step and 2-step optimization.

L_b is the Markstein length that correlates the effect of the stretch to the flame speed evolution and accounts for the flame stretch sensitivity. Finally, the unstretched laminar burning velocity S_L^0 is determined from the unstretched laminar flame propagation velocity by introducing the expansion factor ρ_b/ρ_u

$$S_L^0 = \frac{\rho_b}{\rho_u} V_S^0 \qquad (6)$$

Where the expansion factor is estimated by computing the burned and unburned densities through the EQUIL code from CHEMKIN package [39]. Due to the difficulty to implement the correct gasoline composition in the chemical equilibrium software, the chemical composition of the TRF-E can be used for the computation of the gasoline laminar burning velocity. This approximation will be justified in the results section, comparing the similar dynamic behavior of the two fuels (i.e. flame propagation speed dependence on stretch rate).

4. Mathematical Correlation

Initially proposed by Metghalchi and Keck [34] and widely used in the literature, the mathematical correlation aims to predict the laminar burning velocity of a specific fuel starting from the mixture and thermodynamic parameters. This means that it is possible to write a relationship such that $S_L^0 = (T_i, P_i, \phi)$, corresponding to the

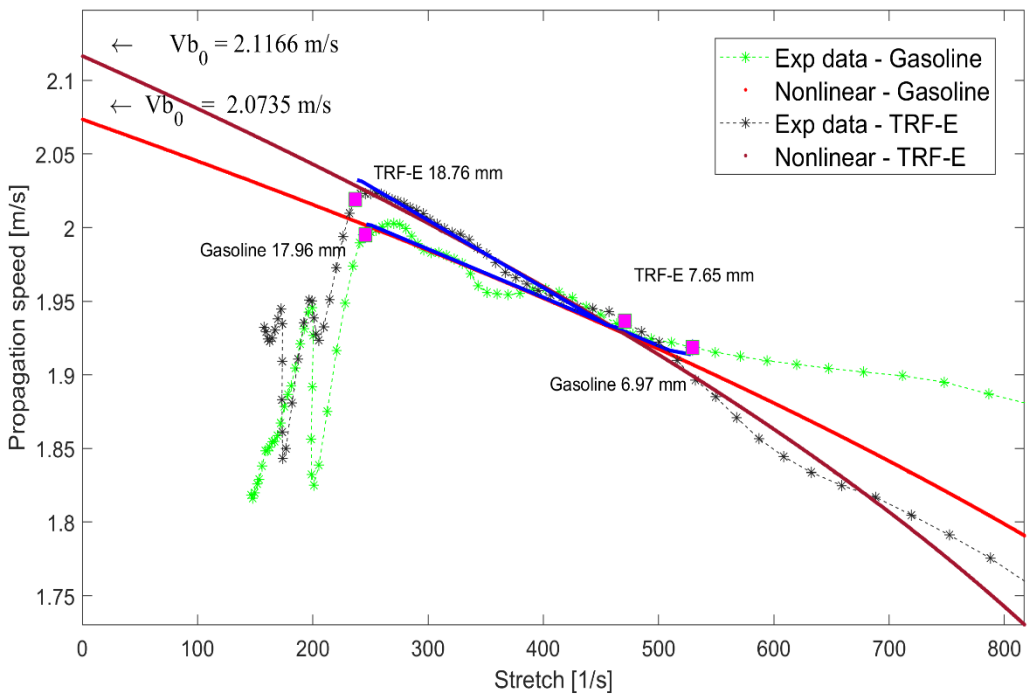

Figure 4: TRF-E and gasoline propagation speed function of stretch rate. The data are extrapolated from test performed at pressure of 3 bar, dilution of 10% EGR and temperature of 473 K. Experimental data are reported as well as nonlinear Kelly and Law correlation. Extrapolated unstretched propagation speed and radii range analyzed are reported.

explicit form

$$S_L^0 = S_{Lref}^0 \left(\frac{T_i}{T_{ref}}\right)^{\alpha_S} \left(\frac{P_i}{P_{ref}}\right)^{\beta_S} \qquad (7)$$

Where T_{ref} and P_{ref} are respectively the reference temperature and the pressure and S_{Lref}^0 the laminar burning velocity under these conditions (expressed in cm/s). Then, the terms S_{Lref}^0, α_S and β_S are a function of the equivalence ratio ϕ, hence

$$S_{Lref}^0 = A + B(\phi - \phi_m) + C(\phi - \phi_m)^2 \qquad (8)$$

$$\alpha_S = \alpha_0 + \alpha_1(\phi - \phi_m) \qquad (9)$$

$$\beta_S = \beta_0 + \beta_1(\phi - \phi_m) \qquad (10)$$

with ϕ_m representing the reference equivalence ratio equal to 1.1.

Nevertheless, according to Varea et al. [40], the pressure dependence is not linear and, thus, the pressure term evolves following a quadratic law yielding to a different equation of the exponent β_S, that is

$$\beta_S = \beta_0 + \beta_1(\phi - \phi_m) + \beta_2(\phi - \phi_m)^2. \qquad (11)$$

Galmiche et al. [7] proposed to implement the effect of dilution by adding a third term and, thus, a new exponent is introduced

$$\gamma_S = \gamma_0 + \gamma_1(\phi - \phi_m) \qquad (12)$$

Then, the complete relationship is

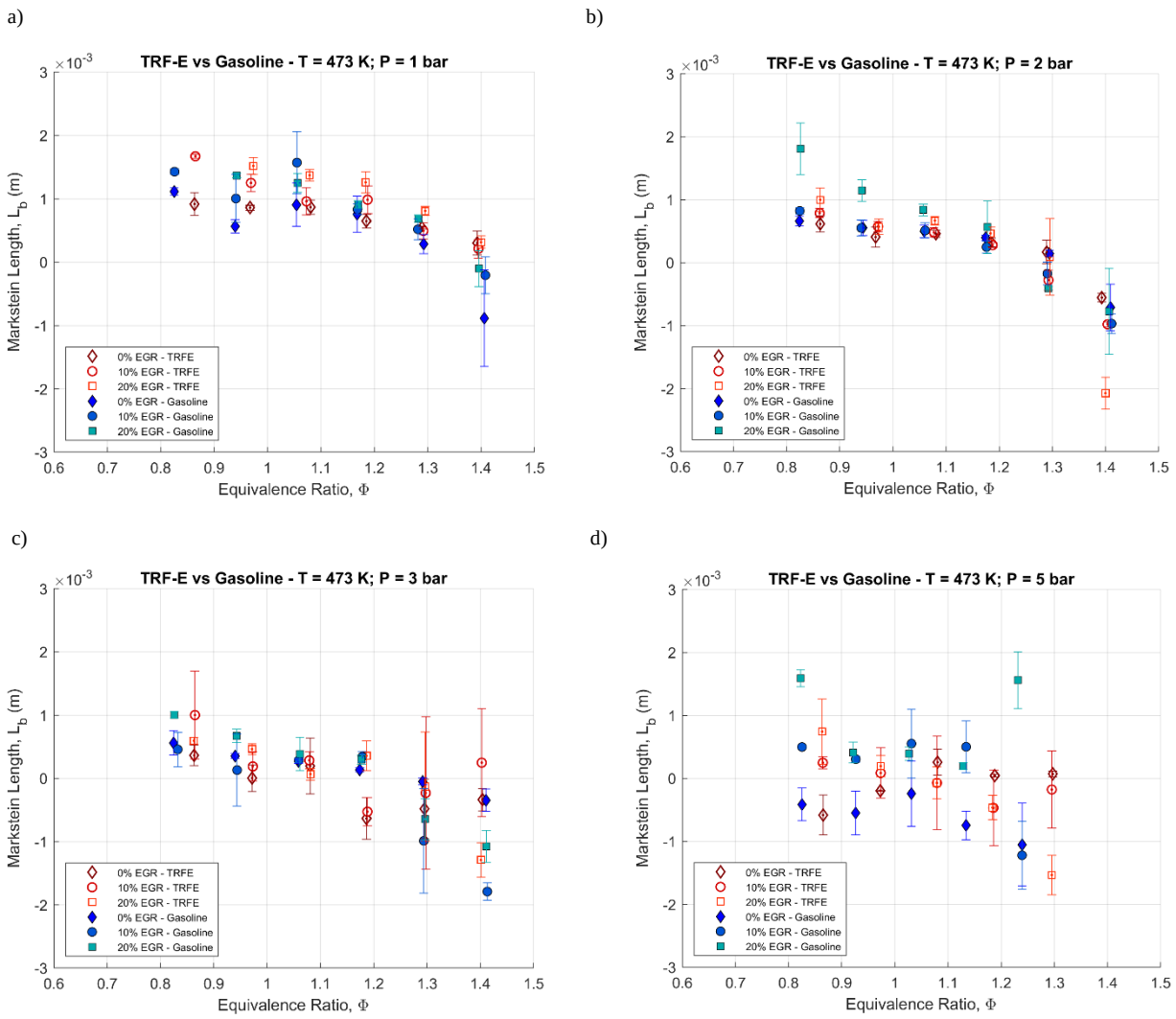

Figure 5: TRF-E and gasoline Markstein lengths comparison at different pressure values (Figures a, b, c, d) and fixed temperature (T = 473 K) for three dilution rates.

$$S_L^0 = S_{Lref}^0 \left(\frac{T_i}{T_{ref}}\right)^{\alpha_S} \left(\frac{P_i}{P_{ref}}\right)^{\beta_S} \left(\frac{\upsilon_{O_2 i}}{\upsilon_{O_2 ref}}\right)^{\gamma_S}. \qquad (13)$$

In this new correlation the term υ_{O_2} takes into account the percentage of oxygen in the global mixture of synthetic air and diluent, thus

$$\upsilon_{O_2} = \frac{n_{O_2(air)}}{n_{O_2(air)} + n_{N_2(air)} + n_{(diluent)}} \times 100 \qquad (14)$$

where *n* refers to the number of moles of the different mixture components.

The global optimization consists in resolving the minimization problem in which the objective function is the mean squared error between the experimental data and the correlation (13). In order to find all the coefficients the optimization process is developed in two phases:

- First, the coefficients A, B and C are determined under the reference conditions, therefore only the relative experimental data are taken into account;
- In the second phase are then included all the other points. In this way it is possible to compute the coefficients that appear in Eq. 9, Eq. 11 and Eq. 12, obtaining the exponents α_S, β_S and γ_S.

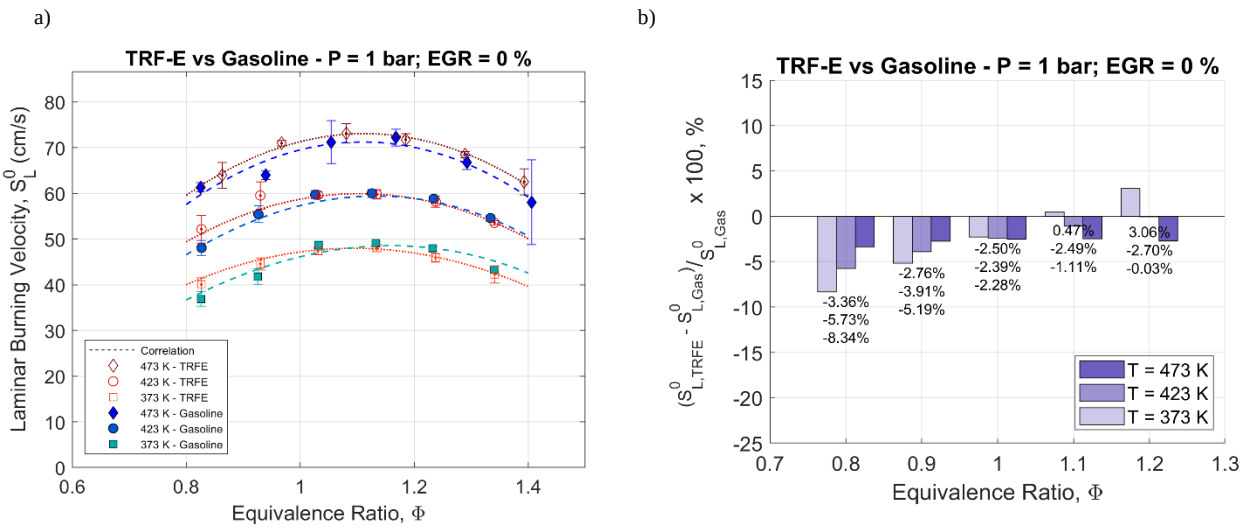

Figure 6: TRF-E and gasoline laminar burning velocities comparison at 1 bar initial pressure without dilution for three initial temperature conditions..

Moreover, in the present study, the optimization process is performed in two steps for both the procedures just discussed. In other words, starting from a generic initial guess (*e.g.* a vector of zeroes) a raw solution is calculated and, successively, this is used as initial guess for a second iterative process. It was found that for the coefficient A, B and C this procedure is redundant, as the algorithm converges to the final optimized solution also with the first generic initial guess. On the contrary, the determination of the exponents is strongly affected by the 2-step process leading to a significant difference of the results. The difference between the 1-step and the 2-step derived coefficients is illustrated in Figure 3. The figure highlights the enhancement of accuracy of the 2-step coefficients, in particular for rich mixtures. Anyway, it was observed that any further iterative process led to the same problem solution obtained at the second step, independently on the initial generic guess of the first step. The results of this investigation are reported in

Table 3 and Table 4. The TRF-E coefficients are further refined by extending the experimental matrix. Other two temperatures were investigated, combining the full range of considered dilution and pressure.

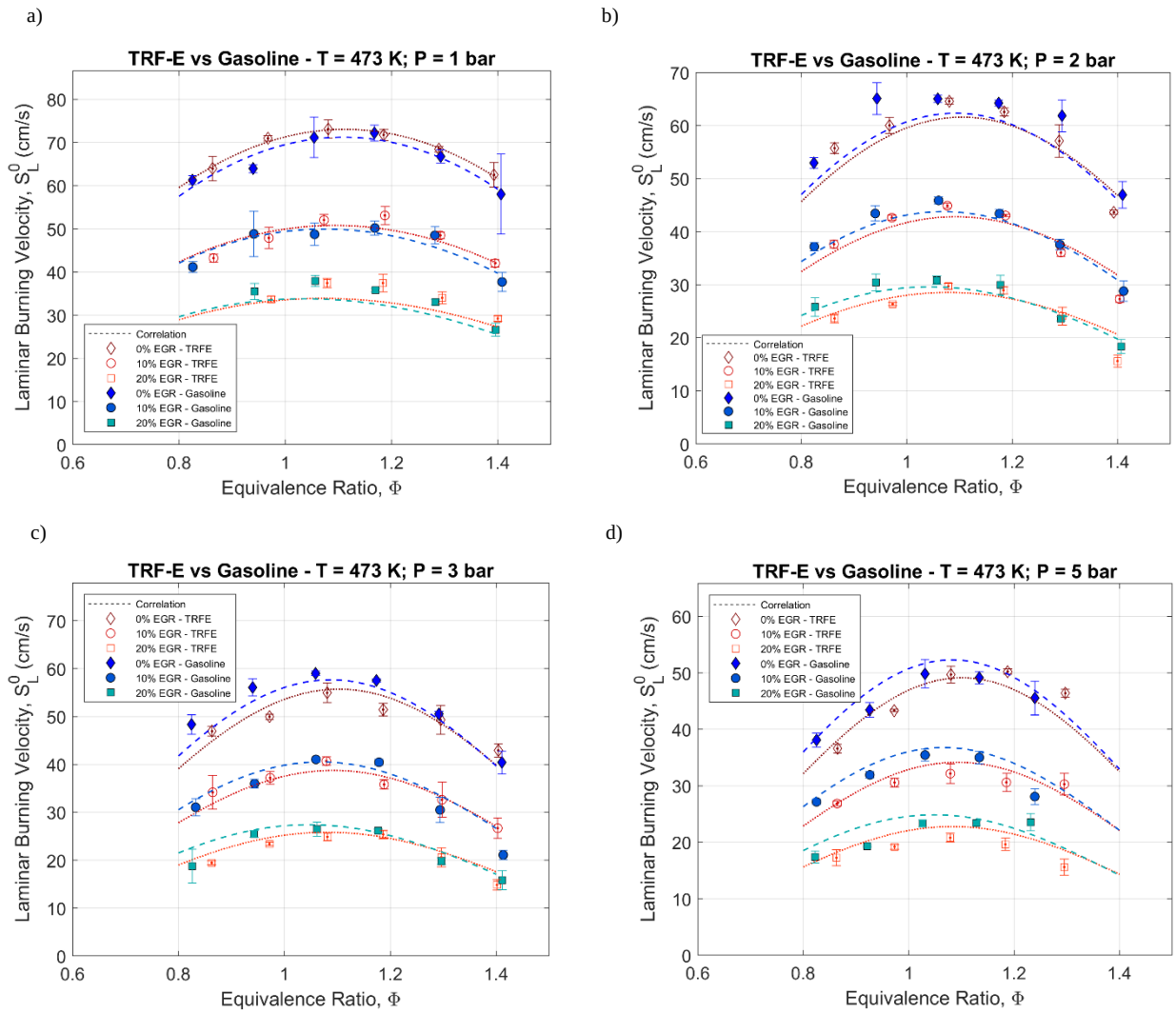

Figure 7: TRF-E and gasoline laminar burning velocities comparison at different pressure values (Figures a, b, c, d) and fixed temperature (T = 473 K) for three dilution rates.

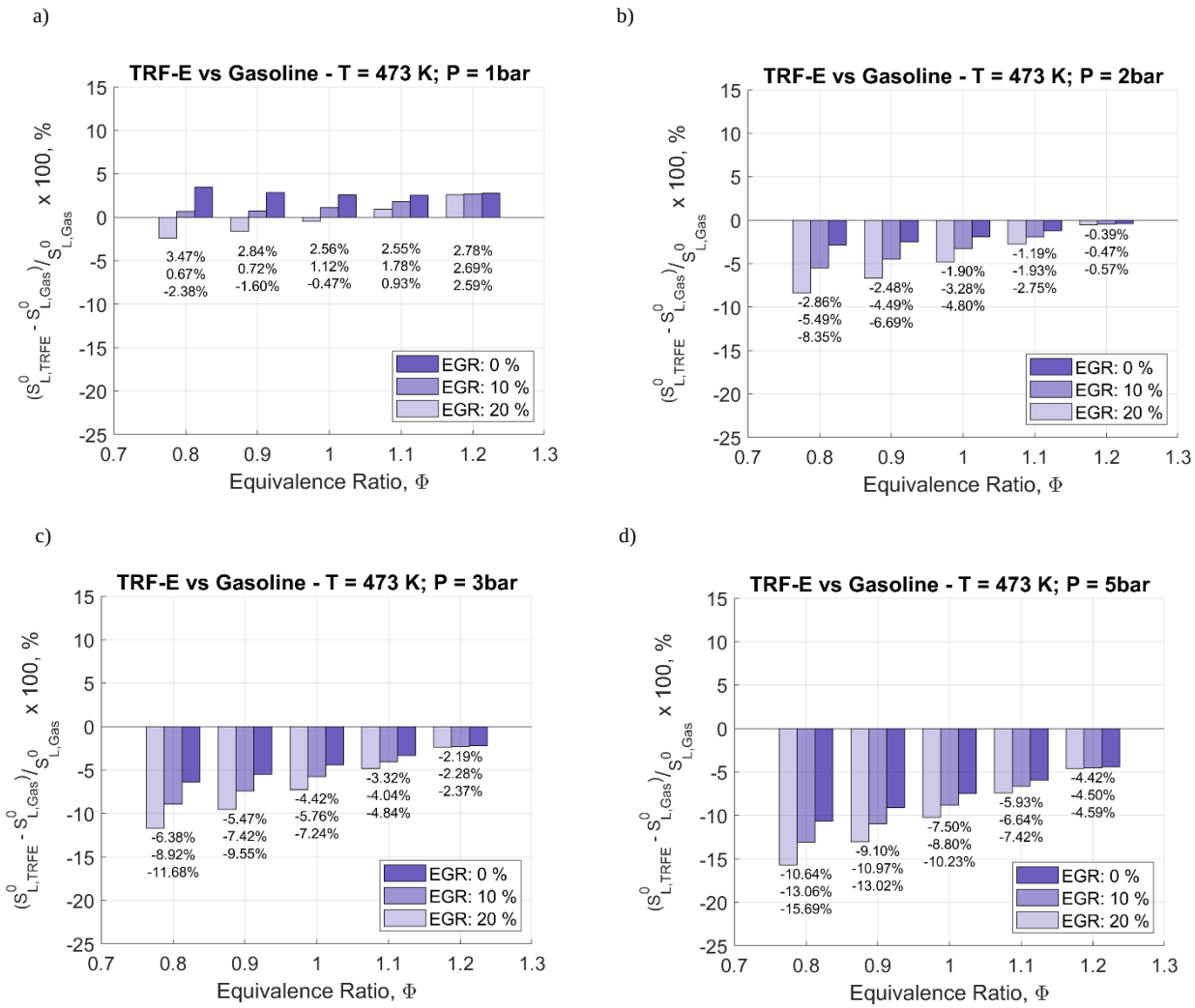

Figure 8: TRF-E and gasoline laminar burning velocities difference at different equivalence ratio for increasing pressure (Figures a, b, c, d) and dilution (EGR = 0, 10, 20 %) at fixed temperature (T = 473 K).

5. Results and Discussion

For what concerns the laminar burning velocities extrapolation, as discussed in the previous sections the data reliability must be evaluated in terms of both post-process uncertainties and experimental limits (*e.g.* misfire due to high dilution percentage at low temperature and/or pressure that reduce the flammability limits, or cellularity due to high equivalence ratio and relatively high pressure and/or low temperature). Among these latter, the use of the non-linear equation previously introduced yields more precise results with respect to the linear one, especially when the burned gases' Markstein length reaches or exceeds the unity [38]. As discussed in the Section 3, ignition effect and wall influence reduce the range of the radii (6.5 – 25 mm). The arising of early cellularity for high equivalence ratio and relatively high pressure and/or may further reduce this range [19]. Moreover, the contour

detection scripts may introduce subsequent errors that must be taken into account. For all these reasons, it is important to remark that the error bars displayed in the following subsections will be representative not only of the corrected standard deviation but also of the post-process uncertainties introduced [41], and are computed by adding the different uncertainties *in quadrature.*

$$err_{tot} = \sqrt{(err_{post-process})^2 + (err_{statistic})^2} \ . \qquad (15)$$

5.1. TRF-E Validation as gasoline surrogate

In order to evaluate how the TRF-E surrogate fits the properties of the investigated gasoline, the comparison of the different laminar burning velocities is performed under several experimental conditions as seen in Table 2. In particular, the accordance between the two fuels must be evaluated under reference conditions and, then, by

Coefficient	Optimized value – Gasoline		Optimized value – TRF-E	
	1-step	***2-step***	***1-step***	***2-step***
A	71.2043	71.2043	73.0208	73.0208
B	2.7185	2.7185	3.5315	3.5315
C	-142.8526	-142.8526	-138.1265	-138.1265
$\boldsymbol{\alpha_0}$	0.8259	1.6437	1.4977	1.7696
$\boldsymbol{\alpha_1}$	-0.7370	-0.8478	-1.1148	0.3151
$\boldsymbol{\beta_0}$	-0.17857	-0.1926	-0.2325	-0.2463
$\boldsymbol{\beta_1}$	-0.2150	-0.1195	-0.0428	-0.0242
$\boldsymbol{\beta_2}$	-2.0643	-1.5001	-2.2700	-1.5983
$\boldsymbol{\gamma_0}$	3.3959	3.3782	3.4994	3.4494
$\boldsymbol{\gamma_1}$	-0.1844	1.3476	-0.0872	0.7151

Table 3: Mathematical correlation coefficients (relative to the laminar burning velocity) for both TRF-E and gasoline determined at fixed temperature and different values of equivalence ratio, pressure and dilution. Coefficients A, B, C refer to the equivalence ratio fitting equation at reference conditions. First column of each fuel displays the classic one-step method that solves the global optimization problem only once. The second column consists of a further system resolution using the 1-step coefficients as initial guess.

Coefficient	Optimized value – TRF-E (without temperature variation)		Optimized value – TRF-E (with temperature variation)	
	1-step	***2-step***	***1-step***	***2-step***
A	73.0208	73.0208	73.0208	73.0208
B	3.5315	3.5315	3.5315	3.5315
C	-138.1265	-138.1265	-138.1265	-138.1265
$\boldsymbol{\alpha_0}$	1.4977	1.7696	1.7702	1.7495
$\boldsymbol{\alpha_1}$	-1.1148	0.3151	-1.2579	-0.1010
$\boldsymbol{\beta_0}$	-0.2325	-0.2463	-0.2453	-0.2481
$\boldsymbol{\beta_1}$	-0.0428	-0.0242	-0.1499	0.0232
$\boldsymbol{\beta_2}$	-2.2700	-1.5983	-1.7451	-1.7739
$\boldsymbol{\gamma_0}$	3.4994	3.4494	3.5018	3.4143
$\boldsymbol{\gamma_1}$	-0.0872	0.7151	-1.9900	0.4252

Table 4: Mathematical correlation coefficients (relative to the laminar burning velocity) for TRF-E fuel determined at fixed temperature and different values of equivalence ratio, pressure and dilution firstly, and then including temperature variation in the global optimization problem. Coefficients A, B, C refer to the equivalence ratio fitting equation at reference conditions. First column of each fuel displays the classic one-step method that solves the global optimization problem only once. The second column consists of a further system resolution using the 1-step coefficients as initial guess.

changing the relevant parameters. This will allow appreciating how the surrogate responds to this variation and how it "follows" the gasoline behavior, quantifying the differences.

As introduced in the previous section, an error is normally introduced in the calculation of the gasoline expansion factor using the TRF-E composition. Anyway, evaluating the dynamic behavior of the two fuels (that is, the propagation speed as function of the stretch rate and, thus, the Markstein length) it is possible the strength of this approximation. Figure 4 reports the stretched propagation speed as function of the stretch rate for both the TRF-E and the gasoline, for one representative condition ($T = 473\ K, \mathrm{P} = 0.3$ MPa, $\phi = 1.0$ and 10% EGR). It

seems clear that, in this case, the dynamic behavior of TRF-E and gasoline is similar. Figure 5 summarizes the comparison between Markstein lengths of the two fuels under the investigated conditions. Figure 5 (a) and (b) evidence a very good agreement between TRF-E and gasoline for every equivalence ratio. With increasing pressure, anyway, the Markstein length determination becomes tougher. Figure 5 (c) highlights points scattering in the rich zone, with also large error bar, while Figure 5 (d) presents large uncertainties over all the equivalence ratio range. However, at the end of this consideration, it has sense to assume that the error in the computation of the expansion factor could be negligible since the two fuels exhibit similar dynamic behavior.

According to Figure , under reference conditions ($T_{ref}, P_{ref}, EGR_{ref}$), the laminar burning velocity of TRF-E with respect to gasoline is in a relative short interval (-2.70 %, -3.36 %, see Figure Figure (b)) among all investigated ER range. On the other hand, decreasing temperature affects the laminar burning velocity of the two fuels in a different way. In fact, though the TRF-E shows a constant lowering for all ER values, maintaining the same curve shape, the gasoline exhibits a stronger slowdown in lean conditions with respect to the rich zone that, on the contrary, seems to be less influenced. That corresponds to a change in the curve shape and a slight shifting of the maximum gasoline S_L^0 value to higher ER. As seen in Figure (a), at $T = 423\ K$, gasoline laminar burning velocity is still lower than the TRF-E one for lean mixtures. The laminar burning velocity of the two fuels is similar after ϕ = 1.1. On the contrary, at $T = 373\ K$, after ϕ = 1.1, gasoline rich mixtures are faster than TRF-E ones. Figure (b) quantifies the gap between the two fuels at $T = 373\ K, 423$ K and 473 K.

Figure displays the laminar burning velocities of the two fuels for all different investigated pressures by varying the dilution rate at fixed temperature ($T = 473\ K$). Increasing EGR rate produces an opposite effect with respect to the previously discussed temperature reduction. Therefore, the leaner is the gasoline mixture, the less it is influenced by the increase of dilution. This leads to the trend inversion with respect to temperature case as highlighted in Figure (a-b). This behavior induces an intersection of the two fuels curves, as seen in Figure (b), as the TRF-E is equally affected within all the ER range. For the other graphs, that is, Figure (c-d), this phenomenon is partially hidden by the pressure influence. In fact, increasing pressure decreases significantly the laminar burning velocity more strongly for TRF-E than for gasoline, independently of the ER (in Figure (d) TRF-E has become slower than gasoline among the whole ER range). As reported in Figure (a-d) the combination of dilution rate and pressure increase leads to an appreciable difference between the laminar burning velocities of the two fuels for lean

mixtures. On the contrary, this discrepancy is less evident for increasing ϕ values. The gap between the two fuels is quantified in Figure, where the dependency on the ER is also put in emphasis.

The mathematical correlation, as observed in the graphs reported in the present section, leads to quite precise results evidencing a good predictability of the fuels behavior. As expected, the hardest conditions underlie the largest discrepancies, that is, high pressure or high dilution rate or the combination of both (Figure (d)). The optimized coefficients are reported in

Table 3, for both the 1-step and the 2-step coefficients. The fact that the gasoline and TRF-E coefficient are significantly close supports the appreciable properties of the TRF-E as gasoline surrogate. This is also confirmed by the accordance of the experimental data under the great part of the investigated conditions, evidencing large discrepancy in the laminar burning velocity values only under the hardest condition (high dilution and pressure and low equivalence ratio). Anyway, this gap is limited to ~15 % in the worst cases (see Figure (d)).

5.2 TRFE extended condition

Once the direct comparison between the gasoline and its surrogate was performed and critically analyzed, the experimental conditions grid was extended for the TRF-E in order to increase the mathematical correlation precision and enlarge the data availability for future kinetic model development. Table 4 shows the coefficients obtained at fixed temperature but with pressure and dilution variations and the ones computed by solving the enlarged global optimization problem (that is, taking into account all the combinations with temperature variation in addition). Figure shows the TRF-E laminar burning velocities under the investigated conditions. In particular, for sake of clearance, the temperature and dilution variation curves are reported for each different considered pressure. This approach points out several evidences. First, for what concerns the experimental investigation it is possible to notice that for some limit conditions there is a lack of experimental points. For example, at low pressure and temperature and high dilution rate ignition problems could be experienced leading to a reduction of the ER investigated range. This could also affects the quality of the global optimization due to a non-uniform number of points for the different thermodynamic conditions. At the same time, during the post-processing, other issues could limit the meaningful radii that it is possible to consider, avoiding thermo-diffusive instabilities. A concurrency effect of high pressure, low temperature and high equivalence ratio leads to an early cellularity arising and, thus, to a lack of exploitable points under certain equivalence ratios, as can be seen in Figure . The result is that the great

part of collected data is in the lean zone for certain parameters combinations. Despite this, once again the correlation seems to adequately fit the experimental data even though a not negligible overestimation is observed for 10 and 20 % dilution rate at 3 and 5 bar when the temperature is 423 or 473 K (Figure (c-d)). On the contrary, lower pressure (that is, 1 and 2 bar) may lead to a slight underestimation for 20 % of dilution rate (Figure (a-b)). Figure 10 summarizes these differences in terms of absolute error of the laminar burning velocity correlation with respect to the experimental data. The bars height and color proportionally depend on the error entity. Each combination of dilution and pressure is reported, considering three equivalence ratio (1.0, 1.1, 1.2). Figure 10 (a) illustrates the fitting quality at $T = 373\ K$ in which the major differences are obtained for 0.2 MPa and 20% dilution and 0.5 MPa and 10% dilution. Beside these cases the error is limited to 6-7%. On the contrary, at $T = 423\ K$, the average error at low (10%) or zero dilution is lower except for pressure of 0.2 MPa ($\phi = 1.2$) and 0.3 MPa ($\phi = 1.1 - 1.2$). At 20% dilution, and pressure higher than atmospheric, error is still around 10%. Finally Figure 10 (c) reports results at $T = 473\ K$ (that is, reference temperature). In this case the error is generally low (less than 6%) except for a case at 20% dilution and 0.1 MPa and all the considered equivalence ratios at 20% and 0.5 MPa (error around 12%).

6. Conclusions

A deep investigation on the laminar burning velocities of two fuels was performed. In the present work, a wide database is set up for a pure gasoline (*B71 1188 ESSH EURO5 +20, RON 96.6 MON 86.2, Ethanol 5%vol*) and its four-components surrogate named TRF-E. Markstein lengths of the two fuels were also analyzed and compared. It was found that the Markstein length trend is similar over an appreciable range of experimental conditions. The comparison lacks in precision just at relatively high values of pressure. In fact, at 0.3 MPa, and for rich mixtures, negative Markstein lengths can be observed for both fuels with large error bars. In addition, at 0.5 MPa the direct comparison of the Markstein length is even more complex due to the uncertainties in the determination of the gasoline Markstein length at 10% or 20% dilution. Despite this, dynamic behavior of the two fuels (i.e., propagation speed dependence on stretch rate) is similar. Moreover, it was observed a good agreement of the laminar burning velocity values. Over a wide range of pressure, dilution and temperature, the difference in laminar burning velocity between gasoline and TRF-E is limited at ~ 15% for the worst case (0.5 MPa, 473 K, 20% EGR and 0.8 equivalence

ratio). In general, the major divergence between the behavior of the two fuels is caused by the pressure increase. The effect of dilution is low, highlighting the fact that the TRF-E can replicate the gasoline properties at high dilution rate. Temperature variation, as well, has a similar effect on both the fuels even if a dependence on the equivalence ratio was observed. In fact, it was found out that for $\phi > 1$ the TRF-E properly follows the gasoline response to pressure, temperature and dilution variations. On the contrary, for lean mixtures the differences are accentuated. As a consequence TRF-E is an acceptable surrogate for the exanimated gasoline. Anyway, it has to be remarked that a further increase in pressure (with respect to the investigated 0.5 MPa) may lead to non-negligible difference in laminar burning velocity, in particular for lean mixtures.

The gathered data permitted to determine the optimized coefficients of the well-known mathematical correlation proposed by Metghalchi and Keck [34] and extended by Galmiche et al. [7] to include the dilution rate with an acceptable precision even under experimental conditions far from the reference ones. A further step in this direction is represented by the extended experimental grid for the TRF-E that allowed to additionally refine the optimized coefficients. Moreover, the thoroughness of the investigated experimental points yields an optimal pool for the

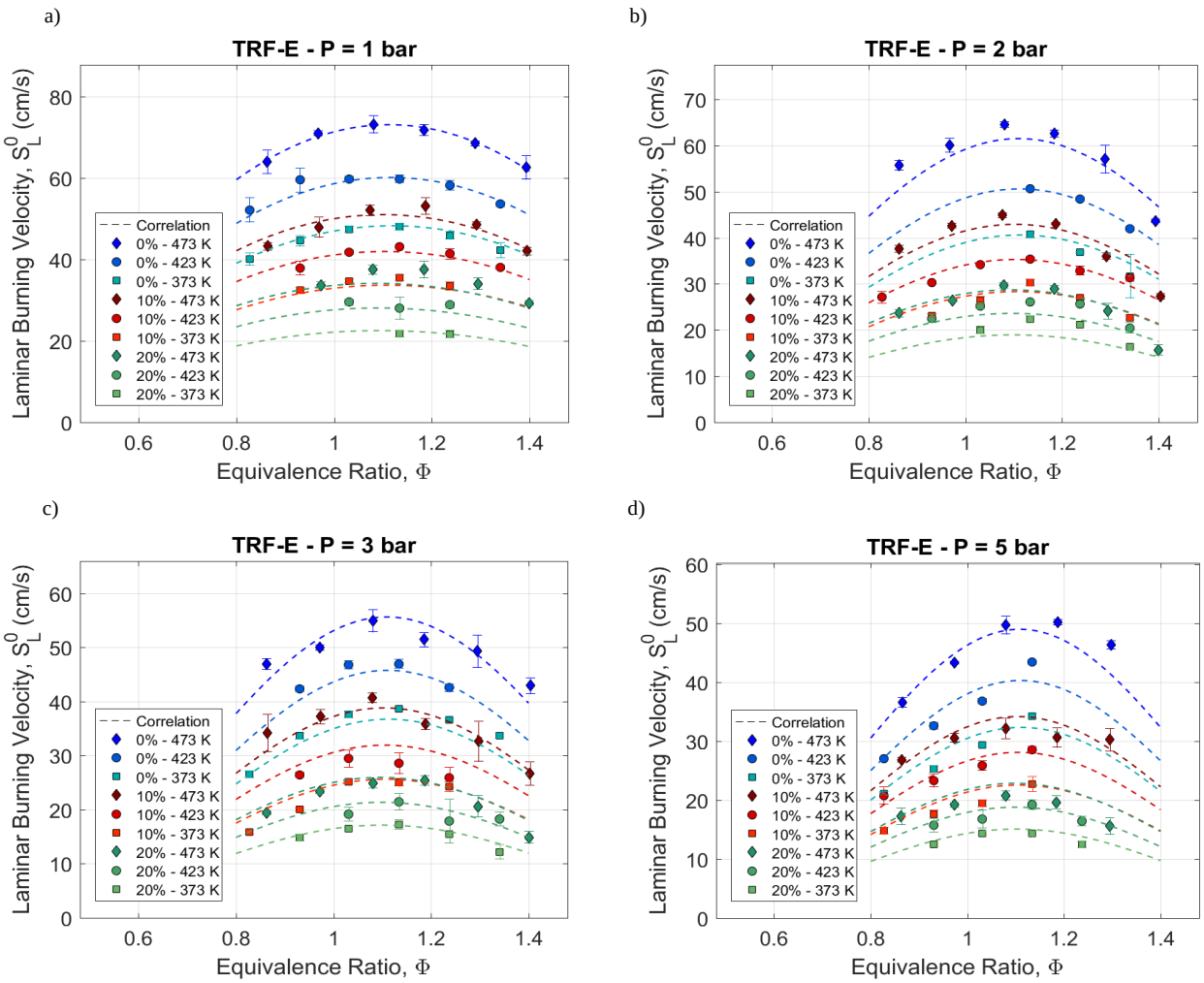

Figure 9: TRF-E laminar burning velocity comparison at different pressure values (Figures a, b, c, d), switching both temperature (T = 373 - 423 - 473 K) and dilution percentages (EGR = 0 - 10 - 20 %)

future development of highly refined chemical kinetic mechanisms. In fact, the database includes not only a wide range of each fundamental parameter (temperature, pressure, dilution rate and equivalence ratio) with respect to the reference conditions, but also a total combination of all their different values within the investigated ranges. The correlation error with respect to the experimental points was evaluated, leading to the conclusion that a good agreement generally exists among the great part of the investigated conditions.

6.1 Next Future Work

Exploiting the huge amount of data gathered during this investigation, next steps will consist of developing of the TRF-E kinetic mechanism.

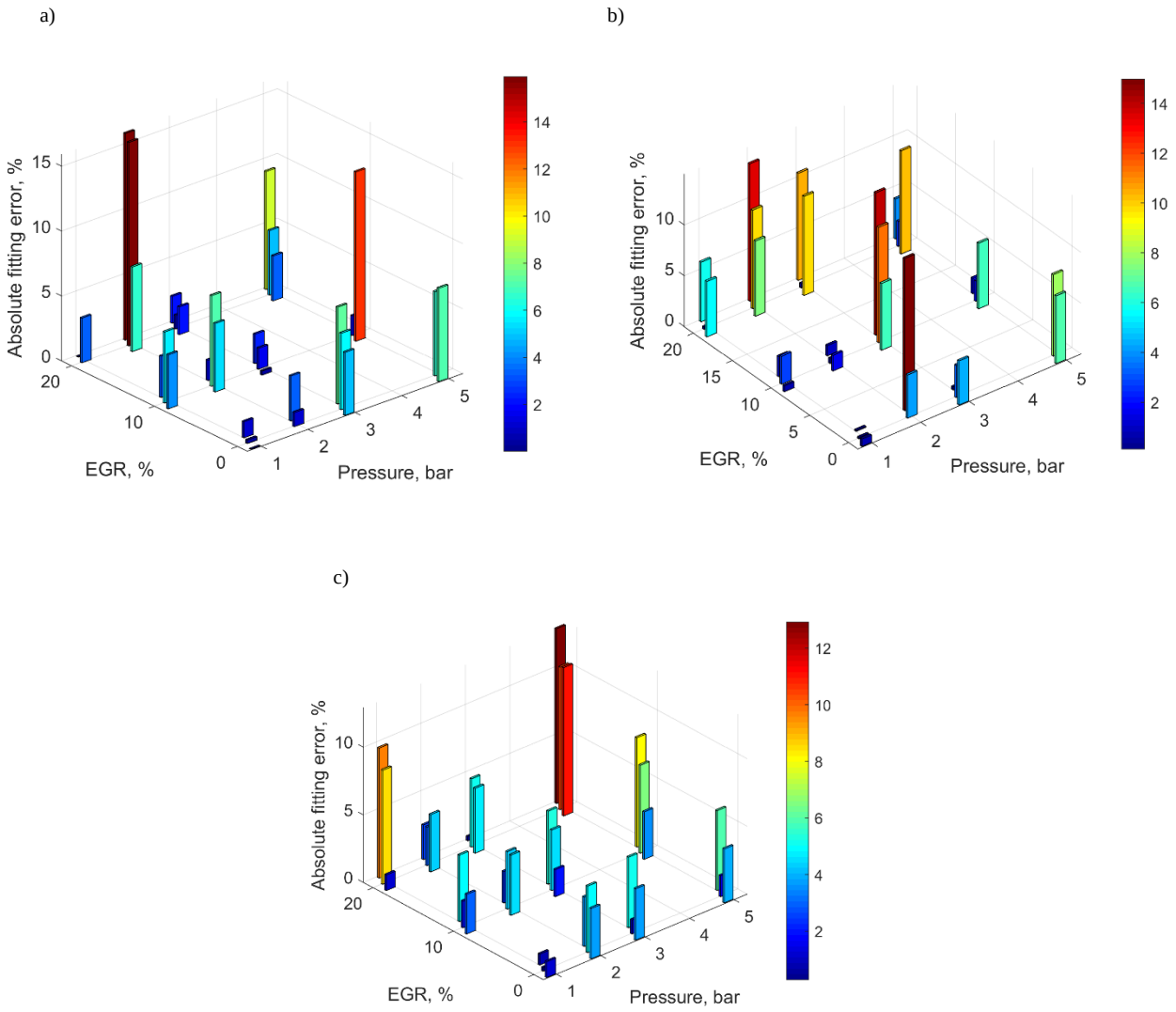

Figure 10: TRF-E laminar burning velocity comparison between experimental points and correlation at three different temperatures (T = 373 (a) – 423 (b) – 473 (c) K). Each plot reports the absolute value of the percentage error between the experimental point and the correlation fitting for each combination of pressure and dilution. Both color and height of the bar are representative of the entity of the error. Moreover, for each points (X,Y) three bars are present: the one at the forefront correspond to an ER of 1.0, the intermediate to an ER of 1.1 and the last to an ER of 1.2. Where bar is missing no experimental point is available.

In addition to this path, the experimental conditions will be extended in terms of pressure, temperature and dilution, using another experimental set-up, in order to extend the validity of the mathematical correlation.

ACKNOLEDGEMENTS

This work was supported by the Agence National de la Recherche (ANR) in the MACDIL ("Moteur à Allumage Commandé à fort taux de DILution") project.

REFERENCES

[1] N. Peters, “Laminar flamelet concepts in turbulent combustion,” *Symp. Combust.*, vol. 21, no. 1, pp. 1231–1250, 1988.

[2] C. Mounaïm-Rousselle, L. Landry, F. Halter, and F. Foucher, “Experimental characteristics of turbulent premixed flame in a boosted Spark-Ignition engine,” *Proc. Combust. Inst.*, vol. 34, no. 2, pp. 2941–2949, 2013.

[3] S. Richard, O. Colin, O. Vermorel, A. Benkenida, C. Angelberger, and D. Veynante, “Towards large eddy simulation of combustion in spark ignition engines,” *Proc. Combust. Inst.*, vol. 31 II, pp. 3059–3066, 2007.

[4] O. Vermorel, S. Richard, O. Colin, C. Angelberger, A. Benkenida, and D. Veynante, “Towards the understanding of cyclic variability in a spark ignited engine using multi-cycle LES,” *Combust. Flame*, vol. 156, no. 8, pp. 1525–1541, 2009.

[5] P. Boudier, S. Henriot, T. Poinsot, and T. Baritaud, “A model for turbulent flame ignition and propagation in spark ignition engines,” *Proc. Combust. Inst.*, vol. 24, no. 1, pp. 503–510, 1992.

[6] O. Colin and A. Benkenida, “3D Modelling of Mixing, Ignition and Combustion Phenomena in Highly Startified Gasoline Engines,” *Ecfm*, vol. 58, no. 1, pp. 47–62, 2003.

[7] B. Galmiche, F. Halter, and F. Foucher, “Effects of high pressure, high temperature and dilution on laminar burning velocities and Markstein lengths of iso-octane/air mixtures,” *Combust. Flame*, vol. 159, no. 11, pp. 3286–3299, 2012.

[8] C. Endouard, F. Halter, C. Chauveau, and F. Foucher, “Effects of CO2, H2O, and Exhaust Gas Recirculation Dilution on Laminar Burning Velocities and Markstein Lengths of Iso-Octane/Air Mixtures,” *Combust. Sci. Technol.*, vol. 188, no. 4–5, pp. 516–528, 2016.

[9] X. Wu, Z. Huang, X. Wang, C. Jin, C. Tang, L. Wei, and C. K. Law, “Laminar Burning Velocities and Flame Instabilities of 2,5-Dimethylfuran-Air Mixtures at Elevated Pressures”, *Combustion and flame*, vol. 158, pp. 539-546. 2011.

[10] P. Brequigny, G. Dayma, F. Halter, C. Mounaïm-Rousselle, T. Dubois, and P. Dagaut, “Laminar burning velocities of premixed nitromethane/air flames: An experimental and kinetic modeling study,” *Proc. Combust. Inst.*, vol. 35, no. 1, pp. 703–710, 2015.

[11] O. Mannaa, M. S. Mansour, W. L. Roberts, and S. H. Chung, “Laminar burning velocities at elevated pressures for gasoline and gasoline surrogates associated with RON,” *Combust. Flame*, vol. 162, no. 6, pp. 2311–2321, 2015.

[12] W. J. Pitz, N. P. Cernansky, F. L. Dryer, F. N. Egolfopoulos, J. T. Farrell, and D. G. Friend, “Development of an Experimental Database and Chemical Kinetic Models for Surrogate Gasoline Fuels,” 2007.

[13] A. P. Cruz, C. Pera, J. Anderlohr, R. Bounaceur, A. P. Cruz, C. Pera, J. Anderlohr, R. Bounaceur, and F. B. A, “A complex chemical kinetic mechanism for the oxidation of gasoline surrogate fuels : n heptane , iso octane and toluene - Mechanism development and validation To cite this version : HAL Id : hal-00370855,” 2009.

[14] T. Edwards, M. Colket, N. Cernansky, F. Dryer, F. Egolfopoulos, D. Friend, E. Law, D. Lenhert, P. Lindstedt, H. Pitsch, A. Sarofim, K. Seshadri, M. Smooke, W. Tsang, and S. Williams, “Development of an Experimental Database and Kinetic Models for Surrogate Jet Fuels,” in *45th AIAA Aerospace Sciences Meeting and Exhibit*, American Institute of Aeronautics and Astronautics, 2007.

[15] R. H. Stanglmaier, C. E. Roberts, D. Mehta, C. Chadwell, J. Corwin Snyder, M. I. Watkins, and N. L. Avery, *Measurement of Laminar Burning Velocity of Multi-Component Fuel Blends for Use in High-Performance SI Engines*. 2003.

[16] R. Bounaceur, O. Herbinet, R. Fournet, P.-A. Glaude, F. Battin-Leclerc, A. Pires da Cruz, M. Yahyaoui, K. Truffin, and G. Moreac, *Modeling The Laminar Flame Speed of Natural Gas and Gasoline Surrogates*, vol. SAE. 2010.

[17] S. Jerzembeck, N. Peters, P. Pepiot-Desjardins, and H. Pitsch, “Laminar burning velocities at high pressure for primary reference fuels and gasoline: Experimental and numerical investigation,” *Combust. Flame*, vol. 156, no. 2, pp. 292–301, 2009.

[18] J. P. J. Van Lipzig, E. J. K. Nilsson, L. P. H. De Goey, and A. A. Konnov, “Laminar burning velocities of n -heptane , iso-octane , ethanol and their binary and tertiary mixtures,” *Fuel*, vol. 90, no. 8, pp. 2773–2781, 2011.

[19] D. Bradley, R. A. Hicks, M. Lawes, C. G. W. Sheppard, and R. Woolley, “The measurement of laminar burning velocities and Markstein numbers for iso-octane-air and iso-octane-n-heptane-air mixtures at

elevated temperatures and pressures in an explosion bomb," *Combust. Flame*, vol. 115, no. 1–2, pp. 126–144, 1998.

[20] J. T. Farrell, R. J. Johnston, and I. P. Androulakis, "Molecular Structure Effects On Laminar Burning Velocities At Elevated Temperature And Pressure," 2004.

[21] L. Sileghem, V. A. Alekseev, J. Vancoillie, K. M. Van Geem, E. J. K. Nilsson, S. Verhelst, and A. A. Konnov, "Laminar burning velocity of gasoline and the gasoline surrogate components iso-octane, n-heptane and toluene," *Fuel*, vol. 112, pp. 355–365, 2013.

[22] D. Bradley, M. Lawes, K. Liu, S. Verhelst, and R. Woolley, "Laminar burning velocities of lean hydrogen – air mixtures at pressures up to 1 . 0 MPa," vol. 149, pp. 162–172, 2007.

[23] S. G. DAVIS and C. K. LAW, "Determination of and Fuel Structure Effects on Laminar Flame Speeds of C1 to C8 Hydrocarbons," *Combust. Sci. Technol.*, vol. 140, no. 1–6, pp. 427–449, Dec. 1998.

[24] P. Dirrenberger, P. A. Glaude, R. Bounaceur, H. Le Gall, A. Pires, A. A. Konnov, and F. Battin-leclerc, "Laminar burning velocity of gasolines with addition of ethanol," *Fuel*, vol. 115, pp. 162–169, 2014.

[25] A. A. Konnov, R. J. Meuwissen, and L. P. H. De Goey, "The temperature dependence of the laminar burning velocity of ethanol flames," *Proc. Combust. Inst.*, vol. 33, no. 1, pp. 1011–1019, 2011.

[26] H. J. Curran, "Developing detailed chemical kinetic mechanisms for fuel combustion," *Proc. Combust. Inst.*, vol. 37, no. 1, pp. 57–81, 2018.

[27] B. Galmiche, F. Halter, F. Foucher, and P. Dagaut, "Effects of Dilution on Laminar Burning Velocity of Premixed Methane / Air Flames," *Energy and Fuels, vol. 25(3), no(3),* pp. 948–954, 2011.

[28] J. Santner, F. L. Dryer, and Y. Ju, "The effects of water dilution on hydrogen, syngas, and ethylene flames at elevated pressure," *Proc. Combust. Inst.*, vol. 34, no. 1, pp. 719–726, 2013.

[29] F. Halter, F. Foucher, L. Landry, and C. Mounaïm-Rousselle, "Effect of Dilution by Nitrogen and/or Carbon Dioxide on Methane and Iso-Octane Air Flames," *Combust. Sci. Technol.*, vol. 181, no. July 2014, pp. 813–827, 2009.

[30] T. Tahtouh, F. Halter, E. Samson, and C. Mouna??m-Rousselle, "Effects of hydrogen addition and nitrogen dilution on the laminar flame characteristics of premixed methane-air flames," *Int. J. Hydrogen Energy*, vol. 34, no. 19, pp. 8329–8338, 2009.

[31] J. X. Zhou, M. Cordier, C. Mounaïm-Rousselle, and F. Foucher, "Experimental estimate of the laminar

burning velocity of iso-octane in oxygen-enriched and CO2-diluted air," *Combust. Flame*, vol. 158, no. 12, pp. 2375–2383, 2011.

[32] S. P. Marshall, S. Taylor, C. R. Stone, T. J. Davies, and R. F. Cracknell, "Laminar burning velocity measurements of liquid fuels at elevated pressures and temperatures with combustion residuals," *Combust. Flame*, vol. 158, no. 10, pp. 1920–1932, 2011.

[33] O. A. Mannaa, M. S. Mansour, W. L. Roberts, and S. H. Chung, "Influence of Ethanol and Exhaust Gas Recirculation on Laminar Burning Behaviors of Fuels for Advanced Combustion Engines (FACE-C) Gasoline and Its Surrogate," *Energy and Fuels*, vol. 31, no. 12, pp. 14104–14115, 2017.

[34] M. Metghalchi and J. C. Keck, "Burning velocities of mixtures of air with methanol, isooctane, and indolene at high pressure and temperature," *Combust. Flame*, vol. 48, no. C, pp. 191–210, 1982.

[35] D. Bradley, P. H. Gaskell, and X. J. Gu, "The modeling of aerodynamic strain rate and flame curvature effects in premixed turbulent combustion," *Symp. Combust.*, vol. 27, no. 1, pp. 849–856, 1998.

[36] S. M. CANDEL and T. J. POINSOT, "Flame Stretch and the Balance Equation for the Flame Area," *Combust. Sci. Technol.*, vol. 70, no. 1–3, pp. 1–15, Mar. 1990.

[37] A. P. Kelley and C. K. Law, "Nonlinear effects in the extraction of laminar flame speeds from expanding spherical flames," *Combust. Flame*, vol. 156, no. 9, pp. 1844–1851, 2009.

[38] F. Halter, T. Tahtouh, and C. Mounaïm-Rousselle, "Nonlinear effects of stretch on the flame front propagation," *Combust. Flame*, vol. 157, no. 10, pp. 1825–1832, 2010.

[39] R. J. K. A.E. Lutz, F.M. Rupley, "Equil: A Chemkin Implementation of Stanjan for Computing Chemical Equilibria, Sandia National Laboratories Livermore, CA 94551." 1992.

[40] E. Varea, V. Modica, B. Renou, and A. Boukhalfa, "*Pressure effects on laminar burning velocities and Markstein lengths for Isooctane–Ethanol–Air mixtures*," *Proc. Combust. Inst.*, vol. 34. 2013.

[41] R. J. Moffat, "Describing the uncertainties in experimental results," *Exp. Therm. Fluid Sci.*, vol. 1, no. 1, pp. 3–17, 1988.